Volume 61
Number 81
18 October 2025
Pages 15689–15904

# ChemComm

Chemical Communications

rsc.li/chemcomm

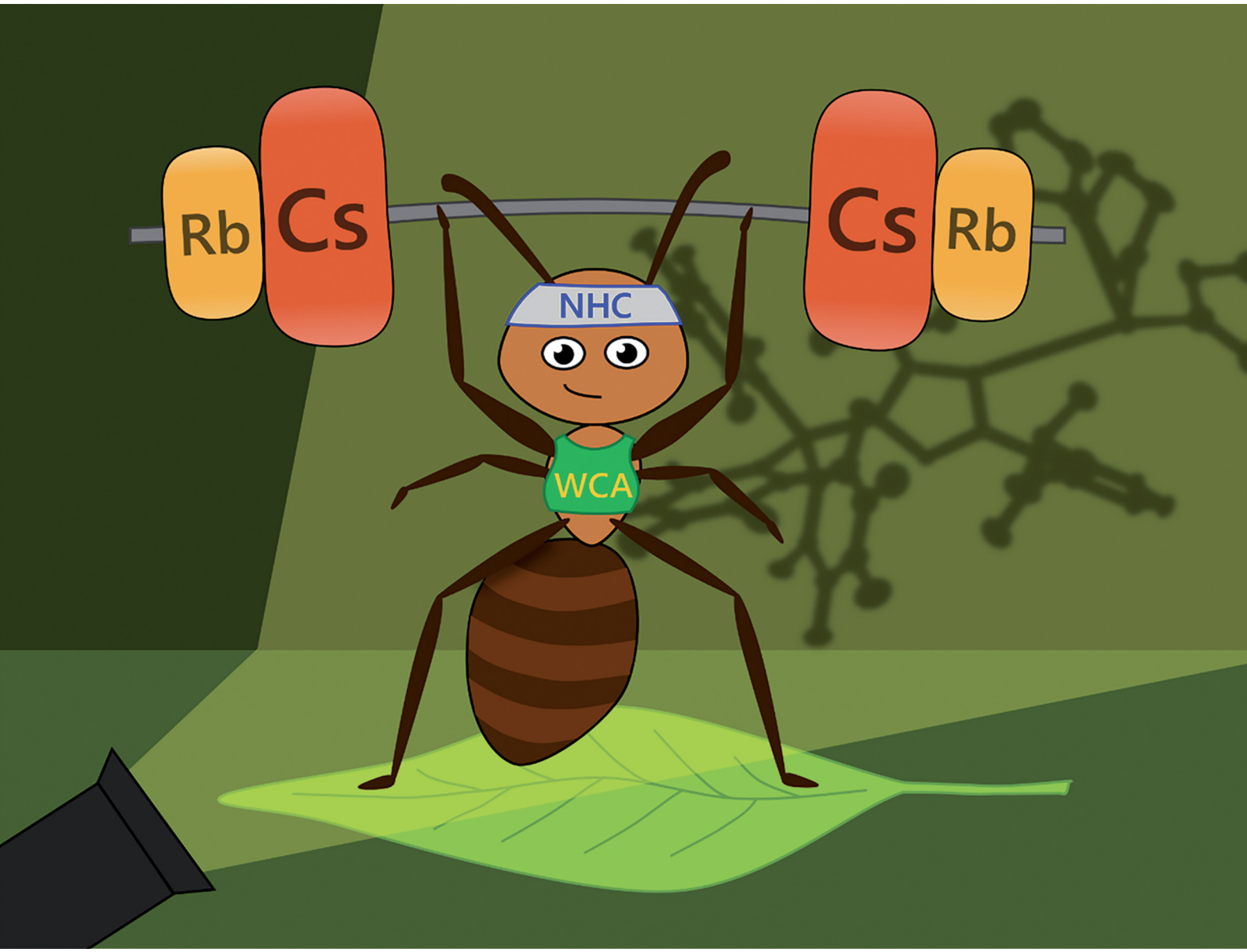


ISSN 1359-7345

ROYAL SOCIETY OF CHEMISTRY

**COMMUNICATION**
Matthias Tamm *et al.*
Heavy alkali metal complexes of N-heterocyclic carbenes

ChemComm

COMMUNICATION

View Article Online
View Journal | View Issue



Cite this: *Chem. Commun.*, 2025, **61**, 15806

Received 7th August 2025,
Accepted 1st September 2025

DOI: 10.1039/d5cc04534g

rsc.li/chemcomm



# Heavy alkali metal complexes of N-heterocyclic carbenes

Lucie J. Groth, Dirk Bockfeld and Matthias Tamm *

**N-Heterocyclic carbene complexes of alkali metals (M = Na, K, Rb, Cs) were prepared from the zwitterionic trimethylsilylimidazolium borate [$(C_6F_5)_3$B(IDipp)SiMe$_3$] (1) by reaction with the corresponding alkali metal *tert*-butoxides MO*t*Bu. The alkali metal complexes were isolated as tetrahydrofuran (THF) solvates of the type [$(C_6F_5)_3$B(IDipp)M(THF)$_x$, 2$^M$(THF)$_x$, and their molecular structures were determined by single-crystal X-ray diffraction analysis.**

N-Heterocyclic carbenes (NHCs) are indispensable ligands in organometallic and coordination chemistry due to their strong σ-donor properties and the high stability of their metal complexes.[1] Since their first isolation as free carbenes,[2] NHCs have been incorporated into complexes with elements across nearly the entire periodic table, including main-group (s- and p-block) elements, transition metals, lanthanides, and actinides.[3–6] Among these, structurally characterised NHC complexes of the heavier alkali metals remain scarce, whereas a considerable number of lithium-NHC complexes have been reported.[3,5,6] Sodium and potassium complexes are also known, particularly those stabilised by ditopic or anionic N-heterocyclic carbenes.[7] However, to the best of our knowledge, no structurally characterised rubidium or caesium NHC complexes have been reported to date.[8] This gap is notable, as heavier alkali metal compounds often exhibit distinct reactivities due to their lower electronegativities, larger ionic radii, and typically higher coordination numbers.[9]

Our group has developed anionic N-heterocyclic carbenes with appended weakly coordinating fluoroborate moieties (WCA-NHCs),[10] which have been extensively used as ancillary ligands in homogeneous catalysis and in main group chemistry.[11–15] In this realm, lithium salts of the type (WCA-NHC)Li(solv.) (solv. = tetrahydrofuran (THF), toluene) have generally been employed as carbene transfer reagents and can be generated from various carbenes, such as 1,3-bis(2,6-diisopropylphenyl)imidazolin-2-ylidene (**IDipp**), by treatment with *n*-butyl lithium,[16] followed by addition of a borane such as tris(pentafluorophenyl)borane, B$(C_6F_5)_3$ (steps 1 and 2 in Scheme 1). This procedure afforded lithium salts containing the lithium-carbene moiety [$(C_6F_5)_3$B(IDipp)Li] (**I**) and crystal structures of **I**(THF)$_2$·0.5toluene and **I**(toluene).[11,15]

Beyond the lithium derivatives, a few sodium and potassium salts have been isolated and structurally characterised, revealing, as expected, larger coordination numbers and a more diverse coordination chemistry. For this purpose, we have employed Lochmann–Schlosser base combinations,[17] which led to the formation of mixed lithium–sodium and lithium–potassium salts in an unpredictable manner.[18] To circumvent the use of lithium organyls, we now describe the reaction of the trimethylsilyl-protected WCA-NHC derivative **1** with alkali metal *tert*-butoxides, M(O*t*Bu) (M = Na, K, Rb, Cs), to form well-defined WCA-NHC complexes **2**$^{Na–Cs}$, all of which were structurally characterised (Scheme 1).

The reaction of the N-heterocyclic carbene **IDipp** with *n*BuLi, followed by addition of B$(C_6F_5)_3$, afforded the well-established lithium salt [$(C_6F_5)_3$B(IDipp)Li(toluene)], **I**(toluene),[13] which

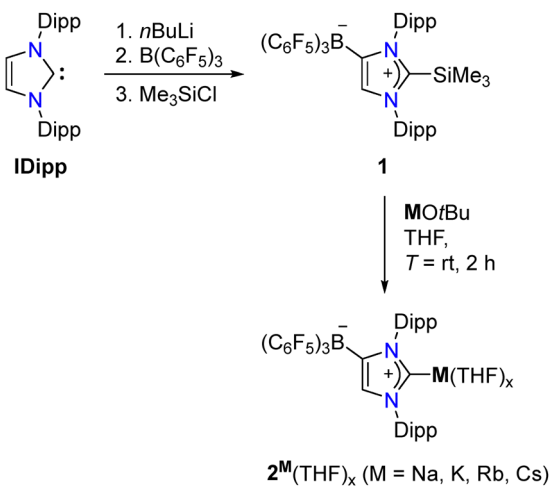


Scheme 1 Synthetic route towards alkali metal NHC complexes.

*Institut für Anorganische und Analytische Chemie, Technische Universität Braunschweig, Hagenring 30, 38106 Braunschweig, Germany.*
*E-mail: m.tamm@tu-bs.de*

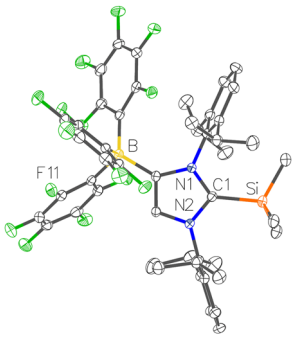


Fig. 1 Molecular structure of **1** with 50% probability displacement ellipsoids. All hydrogen atoms and co-crystallised solvent molecules are omitted for clarity. The unit cell contains four crystallographically independent molecules with identical connectivity. One of these molecules is shown.

was subsequently treated in toluene with trimethylsilyl chloride (TMSCl), in analogy to the procedure reported for the corresponding $BEt_3$ adduct.[19] $[(C_6F_5)_3B(IDipp)SiMe_3]$ (**1**) was isolated as a colourless powder in 49% yield. The $^1H$ and $^{13}C\{^1H\}$ NMR spectra in THF-$d_8$ exhibit broadened signals for the Dipp groups, indicating restricted rotation around the carbene carbon–silicon bond. The characteristic resonance of the C1 carbon atom appears at $\delta$ = 151.5 ppm, within the reported range of 142.0–155.9 ppm for NHC-TMS compounds.[20–22] The $^{19}F\{^1H\}$ NMR shows broad signals at room temperature, which sharpen upon cooling to −50 °C, indicating hindered rotation about the carbon–boron bonds as well. These features suggest that this compound is a promising candidate for use as a carbene transfer reagent *via* desilylation. The $^{29}Si\{^1H\}$ NMR shows one signal at −3.8 ppm.

Single crystals of **1** for X-ray diffraction analysis were obtained by cooling a saturated solution in dichloromethane (DCM)/THF to −40 °C (Fig. 1).[23] The structural parameters are comparable to those of the closely related $[Et_3B(IDipp)SiMe_3]$.[19] Although the steric congestion is evident from the NMR spectra, no significant bending out of the NHC plane is observed, unlike the highly reactive frustrated Lewis pairs (FLPs) featuring *tert*-butyl substituted NHCs.[22] This correlates with the lack of FLP-type reactivity: no reactivity towards $CO_2$ or THF was observed.

To access the alkali metal complexes **2**, we first investigated the reaction of **1** with alkali metal fluorides MF (M = K, Cs) in THF. These reactions proceeded very slowly, and after 24 h afforded only 2% (K) and 15% (Cs) conversion according to $^1H$ NMR spectroscopy. In addition, imidazolium salt formation was observed, which we attribute to the difficulty of obtaining rigorously anhydrous metal fluorides and their poor solubility. We therefore turned to alkali metal *tert*-butoxides MO*t*Bu (M = Na, K, Rb, Cs), which are readily purified by sublimation and provided complexes $\mathbf{2}^{\mathbf{Na–Cs}}$ in fast and clean reactions. After crystallisation from THF/*n*-pentane and drying under vacuum, the compounds were obtained as colourless crystalline solids, which contained varying amounts of THF according to the integrals in their $^1H$ NMR spectra. The yields ranged from 69% to 82%.

The resulting complexes were investigated by NMR spectroscopy in THF-$d_8$. The most characteristic resonance, corresponding to the carbene carbon atom, appears considerably upfield at $\delta$ = 213.7 ppm for $\mathbf{2}^{\mathbf{Na}}$,[18] while the signals for **I** and $\mathbf{2}^{\mathbf{K–Cs}}$ are found at $\delta$ = 217.2 ppm,[11] 217.6 ppm, 216.9 ppm, and 216.2 ppm, respectively. These results contradict the expected trend in which increasing Lewis acidity of the metal leads to an upfield shift of the $C_{carbene}$ resonance, as observed for related complexes containing anionic NHCs such as $[(Me_3SiCH_2)_3Ga(IDipp)M(THF)_3]$ with $\delta$ = 201.5 ppm (M = Li),[24] 202.8 ppm (M = Na), and 210.7 ppm (M = K).[21]

Attempts to obtain suitable single crystals of the complexes $\mathbf{2}^{\mathbf{Na–Cs}}(THF)_x$ were carried out under various conditions and from different solvent mixtures, affording the crystal structures of $\mathbf{2}^{\mathbf{Na}}(THF)_2{\cdot}0.5PhCl$, $\mathbf{2}^{\mathbf{K}}(THF)_2{\cdot}0.5PhCl$, $\mathbf{2}^{\mathbf{K}}(THF)_2{\cdot}0.35THF{\cdot}0.15n$-pentane, $\mathbf{2}^{\mathbf{Rb}}(THF)_2{\cdot}0.5n$-pentane, $\mathbf{2}^{\mathbf{Rb}}(THF)_{2.4}{\cdot}0.6$toluene, and $\mathbf{2}^{\mathbf{Cs}}(THF)_3$. The latter, the caesium complex, crystallised in three polymorphic forms; however, discussion here is confined to one representative polymorph (see SI). An additional rubidium species, $\mathbf{2}^{\mathbf{Rb}}$(THF), was obtained from chlorobenzene and proved to contain an anionic dicarbene-rubidium unit and a separately solvated Rb cation (*vide infra*). All molecular structures are presented in the SI, while representative examples are shown in Fig. 2 and 3.

As expected, the metal–carbene bond lengths in the monocarbene complexes increase steadily from 2.526(3) Å (Na), 2.8708(15)/2.8800(17) Å (K), 3.066(5)/3.078(2) Å (Rb) to 3.3815(16) Å (Cs), reflecting the increasing ionic radius of the alkali metal cation. This series is complemented by corresponding values for lithium and sodium in $\mathbf{I}(THF)_2{\cdot}0.5$toluene and $\mathbf{2}^{\mathbf{Na}}(THF)_3$, namely 2.094(2) Å and 2.5079(18) Å, respectively.[11,18] In contrast to the latter systems, however, all the structures described herein display additional secondary interactions, and in each case, the alkali metal is significantly displaced toward one of the Dipp substituents, with the shortest contact originating consistently from the $C_{ipso}$ carbon atom. These distortions can be attributed to noncovalent cation–π interactions, arising from electrostatic attraction between the cation and the electron-rich π-face of the aryl substituent.[25] It should be noted that similar structural motifs were previously observed for rhodium, iridium and palladium WCA-NHC complexes,[12,13] which served as structurally authenticated examples for the general potential of π-face donation in metal–NHC complexes.[26]

The crystal structures of $\mathbf{2}^{\mathbf{Na}}(THF)_2{\cdot}0.5PhCl$, $\mathbf{2}^{\mathbf{K}}(THF)_2{\cdot}0.5PhCl$, $\mathbf{2}^{\mathbf{K}}(THF)_2{\cdot}0.35THF{\cdot}0.15n$-pentane, and $\mathbf{2}^{\mathbf{Rb}}(THF)_2{\cdot}0.5n$-pentane are isostructural, rendering them particularly suitable for detailed comparison of the structural effects discussed above. Alongside the expected elongation of the NHC-metal bonds (*vide supra*), these complexes exhibit an increasing deviation from the usual linear coordination axis of the NHC ligand. This deviation can be quantified by the inclination of the M–C1 bond relative to the axis defined by the carbene carbon atom C1 and the centroid of the imidazole plane ($Ct_{Im}$): 12.35(16)° (Na), 20.42(9)°/19.94(11)° (K), and 23.4(3)° (Rb). This trend is consistent with progressively stronger cation–π interactions for the larger, softer metals.[27] The coordination spheres are completed by metal–fluorine contacts,

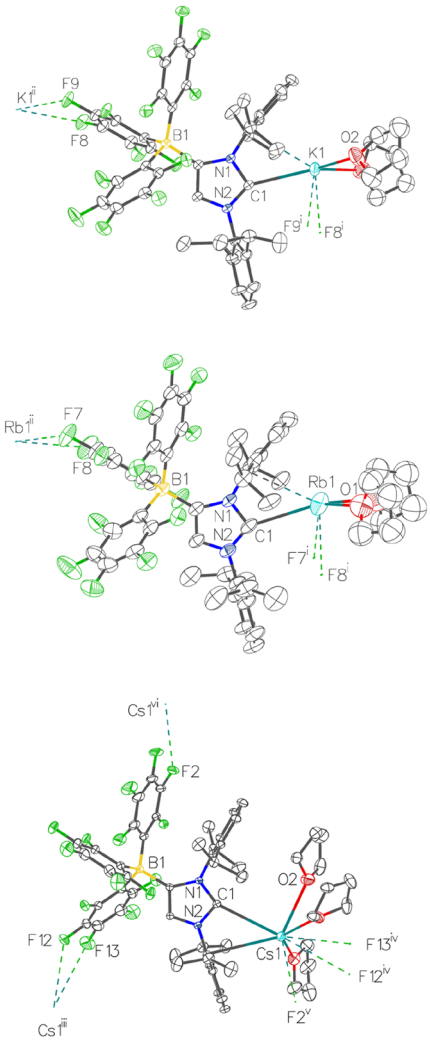


Fig. 2 Molecular structure of $\mathbf{2}^{\mathbf{K}}(THF)_2{\cdot}0.5PhCl$ (top), $\mathbf{2}^{\mathbf{Rb}}(THF)_2{\cdot}0.5n$-pentane (middle) and $\mathbf{2}^{\mathbf{Cs}}(THF)_3$ (bottom) with 50% probability displacement ellipsoids. All hydrogen atoms and cocrystallised solvent molecules are omitted for clarity. Contacts with alkali metal atoms are indicated with stippled lines. The unit cell contains four crystallographically independent molecules with identical connectivity. One of these molecules is shown. Symmetry generated atoms are denoted by (i) $1-x, 1/2+y, 3/2-z$ (ii) $1-x, -1/2+y, 3/2-z$ (iii) $1/2-x, 1/2+y, 1/2+z$ (iv) $1/2-x, -1/2+y, -1/2+z$ (v) $-1/2+x, 1/2-y, +z$ (vi) $1/2+x, 1/2-y, +z$.

with shortest M–F separations of 2.5095(19) Å (Na), 2.8498(12)/2.8539(12) Å (K), 2.980(4) Å (Rb).

As mentioned above, three polymorphs of $\mathbf{2}^{\mathbf{Cs}}(THF)_3$ were identified, all displaying cation–π interactions. Surprisingly, however, in one polymorph the caesium cation does not engage *via* π-face coordination with the Dipp substituent adjacent to the borate moiety; instead, it is displaced by 25.87(10)° toward the opposite Dipp ring. In all three polymorphs, the metal coordination spheres are completed by additional Cs–F contacts, ranging from 3.1722(14) Å to 3.7120(16) Å in the discussed polymorph (Fig. 2, bottom).

For $\mathbf{2}^{\mathbf{Rb}}(THF)$, a dicarbene complex featuring two inequivalent rubidium ions, each located on a crystallographic inversion centre, was obtained (Fig. 3). The rubidium ion Rb1 adopts a

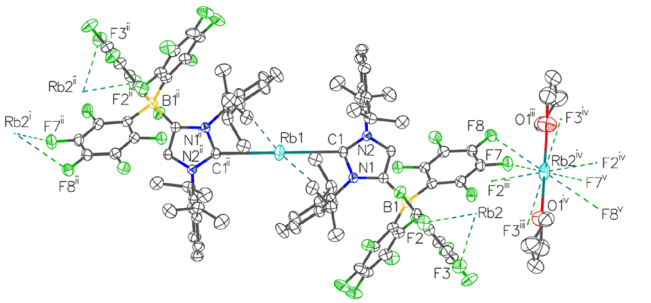


Fig. 3 Molecular structure of $\mathbf{2}^{\mathbf{Rb}}(THF)$ with 50% probability displacement ellipsoids. All hydrogen atoms are omitted for clarity. The unit cell contains four crystallographically independent molecules with identical connectivity. Two of these molecules is shown. Contacts with rubidium atoms are indicated with stippled lines. Symmetry generated atoms are denoted by (i) $1-x, 1-y, 1-z$ (ii) $1-x, 1-y, 1-z$ (iii) $1+x, +y, +z$ (iv) $1-x, 1-y, -z$ (v) $2-x, 1-y, -z$.

linear coordination geometry with two WCA-NHC ligands and additional π-face coordination *via* the borate-flanking Dipp rings, resulting in an inclination of 21.44(12)°, with Rb1–C1 = 2.9845(18) Å and Rb–$C_{ipso}$ = 3.2960(18) Å. In contrast, the second rubidium ion, Rb2, is stabilised solely by coordination of two THF molecules and contacts to the fluoroborate groups, with Rb2–F distances ranging from 2.9609(12) Å to 3.4056(13) Å affording a coordination polymer.

The present study introduces a novel route to alkali metal complexes of borate-decorated anionic N-heterocyclic carbenes (WCA-NHCs) *via* a zwitterionic silylimidazolium borate, culminating in the first structurally verified rubidium and caesium NHC-complexes and completing the series from lithium to caesium. Single-crystal X-ray diffraction analysis confirms a steady increase of M–$C_{carbene}$ bond lengths from Li to Cs, alongside emerging cation–π interactions for the softer, larger metals, as evidenced by pronounced inclination angles and short M···$C_{ipso}$ contacts. These complexes offer promising applications as WCA-NHC transfer reagents, and their alkali metal-dependent nucleophilicity suggests potential utility in catalysis, where the metal counterion may be used to tune reactivity.[28]

L. J. G. carried out the experimental work. D. B. performed the crystallographic analysis. L. J. G. and D. B. drafted the manuscript. M. T. guided the project and revised the manuscript.

This work was financially supported by the Deutsche Forschungsgemeinschaft (DFG) through grants TA 189/9-2 and TA 189/18-1.

## Conflicts of interest

There are no conflicts to declare.

## Data availability

The data supporting this article have been included as part of the SI. Supplementary information: Experimental, analytical

 

and crystallographic details, selected NMR spectra. See DOI: https://doi.org/10.1039/d5cc04534g.

CCDC 2478746–2478754 contain the supplementary crystallographic data for this paper.[29a–i]

## References


1 M. N. Hopkinson, C. Richter, M. Schedler and F. Glorius, *Nature*, 2014, **510**, 485–496.
2 (*a*) A. J. Arduengo, R. L. Harlow and M. Kline, *J. Am. Chem. Soc.*, 1991, **113**, 361–363; (*b*) A. J. Arduengo, H. V. R. Dias, R. L. Harlow and M. Kline, *J. Am. Chem. Soc.*, 1992, **114**, 5530–5534.
3 V. Nesterov, D. Reiter, P. Bag, P. Frisch, R. Holzner, A. Porzelt and S. Inoue, *Chem. Rev.*, 2018, **118**, 9678–9842.
4 (*a*) A. Doddi, M. Peters and M. Tamm, *Chem. Rev.*, 2019, **119**, 6994–7112; (*b*) H. V. Huynh, *The organometallic chemistry of N-heterocyclic carbenes*, Wiley, Hoboken, New Jersey, 2017; (*c*) J. Cheng, L. Wang, P. Wang and L. Deng, *Chem. Rev.*, 2018, **118**, 9930–9987; (*d*) P. L. Arnold and S. T. Liddle, *Chem. Commun.*, 2006, 3959–3971; (*e*) N. Kuhn and A. Al-Sheikh, *Coord. Chem. Rev.*, 2005, **249**, 829–857; (*f*) P. L. Arnold and I. J. Casely, *Chem. Rev.*, 2009, **109**, 3599–3611; (*g*) C. Fliedel, G. Schnee, T. Avilés and S. Dagorne, *Coord. Chem. Rev.*, 2014, **275**, 63–86.
5 S. Bellemin-Laponnaz and S. Dagorne, *Chem. Rev.*, 2014, **114**, 8747–8774.
6 E. Rivard, in *Comprehensive inorganic chemistry II. From elements to applications*, ed. J. Reedijk, Elsevier, Amsterdam, 2nd edn, 2013, pp. 457–484.
7 (*a*) J. B. Waters and J. M. Goicoechea, *Coord. Chem. Rev.*, 2015, **293–294**, 80–94; (*b*) A. Nasr, A. Winkler and M. Tamm, *Coord. Chem. Rev.*, 2016, **316**, 68–124.
8 S. J. Grabowski, *CrystEngComm*, 2023, **25**, 4550–4561.
9 (*a*) C. Schade and P. von Ragué Schleyer, in *Advances in Organometallic Chemistry*, ed. B. W. O'Malley, Academic Press, 1987, vol. 27, pp. 169–278; (*b*) E. Weiss, *Angew. Chem., Int. Ed. Engl.*, 1993, **32**, 1501–1523; (*c*) J. D. Smith, *Adv. Organomet. Chem.*, 1999, **43**, 267–348; (*d*) A. Streitwieser and L. Xie, in *Science of synthesis*, ed. M. Majewski and V. Snieckus, Thieme, Stuttgart, New York, NY, 2006; (*e*) E. Hevia, M. Uzelac and A. M. Borys, in *Comprehensive Organometallic Chemistry IV*, ed. G. F. Parkin, K. Meyer and D. O'Hare, Elsevier, San Diego, 4th edn, 2022, pp. 5–70.
10 L. P. Ho and M. Tamm, *Chem. – Eur. J.*, 2022, **28**, e202200530.
11 S. Kronig, E. Theuergarten, C. G. Daniliuc, P. G. Jones and M. Tamm, *Angew. Chem., Int. Ed.*, 2012, **51**, 3240–3244.
12 E. L. Kolychev, S. Kronig, K. Brandhorst, M. Freytag, P. G. Jones and M. Tamm, *J. Am. Chem. Soc.*, 2013, **135**, 12448–12459.
13 A. Winkler, K. Brandhorst, M. Freytag, P. G. Jones and M. Tamm, *Organometallics*, 2016, **35**, 1160–1169.
14 (*a*) A. Igarashi, E. L. Kolychev, M. Tamm and K. Nomura, *Organometallics*, 2016, **35**, 1778–1784; (*b*) K. Nomura, G. Nagai, A. Nasr, K. Tsutsumi, Y. Kawamoto, K. Koide and M. Tamm, *Organometallics*, 2019, **38**, 3233–3244; (*c*) L. P. Ho, M.-K. Zaretzke, T. Bannenberg and M. Tamm, *Chem. Commun.*, 2019, **55**, 10709–10712; (*d*) K. Nomura, G. Nagai, I. Izawa, T. Mitsudome, M. Tamm and S. Yamazoe, *ACS Omega*, 2019, **4**, 18833–18845; (*e*) J. Frosch, M. Freytag, P. G. Jones and M. Tamm, *J. Organomet. Chem.*, 2020, **918**, 121311; (*f*) L. P. Ho, L. Anders and M. Tamm, *Chem. – Asian J.*, 2020, **15**, 845–851; (*g*) M. Koneczny, L. Phong Ho, A. Nasr, M. Freytag, P. G. Jones and M. Tamm, *Adv. Synth. Catal.*, 2020, **362**, 3857–3863; (*h*) J. Frosch, M. Koneczny, T. Bannenberg and M. Tamm, *Chem. – Eur. J.*, 2021, **27**, 4349–4363; (*i*) L. P. Ho and M. Tamm, *Dalton Trans.*, 2021, **50**, 1202–1205; (*j*) S. Planer, J. Frosch, M. Koneczny, D. Trzybiński, K. Woźniak, K. Grela and M. Tamm, *Chem. – Eur. J.*, 2021, **27**, 15218–15226.
15 L. P. Ho, A. Nasr, P. G. Jones, A. Altun, F. Neese, G. Bistoni and M. Tamm, *Chem. – Eur. J.*, 2018, **24**, 18922–18932.
16 (*a*) A. Jana, R. Azhakar, G. Tavčar, H. W. Roesky, I. Objartel and D. Stalke, *Eur. J. Inorg. Chem.*, 2011, 3686–3689; (*b*) Y. Wang, Y. Xie, M. Y. Abraham, P. Wei, H. F. Schaefer, P. V. R. Schleyer and G. H. Robinson, *J. Am. Chem. Soc.*, 2010, **132**, 14370–14372.
17 (*a*) M. Schlosser, *J. Organomet. Chem.*, 1967, **8**, 9–16; (*b*) L. Lochmann, J. Pospíšil and D. Lím, *Tetrahedron Lett.*, 1966, **2**, 257–262.
18 J. Frosch, L. Körner, M. Koneczny and M. Tamm, *Z. Anorg. Allg. Chem.*, 2021, **647**, 998–1004.
19 Y. Wang, M. Y. Abraham, R. J. Gilliard, P. Wei, J. C. Smith and G. H. Robinson, *Organometallics*, 2012, **31**, 791–793.
20 (*a*) D. Mendoza-Espinosa, B. Donnadieu and G. Bertrand, *J. Am. Chem. Soc.*, 2010, **132**, 7264–7265; (*b*) J. J. Weigand, K.-O. Feldmann and F. D. Henne, *J. Am. Chem. Soc.*, 2010, **132**, 16321–16323; (*c*) A. N. Price and M. J. Cowley, *Chem. – Eur. J.*, 2016, **22**, 6248–6252; (*d*) J. W. Dube, Y. Zheng, W. Thiel and M. Alcarazo, *J. Am. Chem. Soc.*, 2016, **138**, 6869–6877.
21 M. Uzelac, A. R. Kennedy, A. Hernán-Gómez, M. Á. Fuentes and E. Hevia, *Z. Anorg. Allg. Chem.*, 2016, **642**, 1241–1244.
22 M. F. Silva Valverde, E. Theuergarten, T. Bannenberg, M. Freytag, P. G. Jones and M. Tamm, *Dalton Trans.*, 2015, **44**, 9400–9408.
23 P. G. Jones, M. Freytag, H. Ehrhorn and M. Tamm, CCDC 2282386: Experimental Crystal Structure Determination, 2023, DOI: 10.5517/ccdc.csd.cc2gm0ch.
24 M. Uzelac, A. Hernán-Gómez, D. R. Armstrong, A. R. Kennedy and E. Hevia, *Chem. Sci.*, 2015, **6**, 5719–5728.
25 J. C. Ma and D. A. Dougherty, *Chem. Rev.*, 1997, **97**, 1303–1324.
26 R. Credendino, L. Falivene and L. Cavallo, *J. Am. Chem. Soc.*, 2012, **134**, 8127–8135.
27 (*a*) D. Hoffmann, W. Bauer, F. Hampel, N. J. R. van Eikema Hommes, P. von Ragué Schleyer, P. Otto, U. Pieper, D. Stalke, D. S. Wright and R. Snaith,, *J. Am. Chem. Soc.*, 1994, **116**, 528–536; (*b*) U. Pieper and D. Stalke, *Organometallics*, 1993, **12**, 1201–1206; (*c*) D. Hoffmann, W. Bauer, P. von Ragué Schleyer, U. Pieper and D. Stalke,, *Organometallics*, 1993, **12**, 1193–1200.
28 D. Enders, O. Niemeier and A. Henseler, *Chem. Rev.*, 2007, **107**, 5606–5655.
29 (*a*) L. J. Groth, D. Bockfeld and M. Tamm, CCDC 2478746: Experimental Crystal Structure Determination, 2025, DOI: 10.5517/ccdc.csd.cc2p6bkt; (*b*) L. J. Groth, D. Bockfeld and M. Tamm, CCDC 2478747: Experimental Crystal Structure Determination, 2025, DOI: 10.5517/ccdc.csd.cc2p6blv; (*c*) L. J. Groth, D. Bockfeld and M. Tamm, CCDC 2478748: Experimental Crystal Structure Determination, 2025, DOI: 10.5517/ccdc.csd.cc2p6bmw; (*d*) L. J. Groth, D. Bockfeld and M. Tamm, CCDC 2478749: Experimental Crystal Structure Determination, 2025, DOI: 10.5517/ccdc.csd.cc2p6bnx; (*e*) L. J. Groth, D. Bockfeld and M. Tamm, CCDC 2478750: Experimental Crystal Structure Determination , 2025, DOI: 10.5517/ccdc.csd.cc2p6bpy; (*f*) L. J. Groth, D. Bockfeld and M. Tamm, CCDC 2478751: Experimental Crystal Structure Determination, 2025, DOI: 10.5517/ccdc.csd.cc2p6bqz; (*g*) L. J. Groth, D. Bockfeld and M. Tamm, CCDC 2478752: Experimental Crystal Structure Determination, 2025, DOI: 10.5517/ccdc.csd.cc2p6br0; (*h*) L. J. Groth, D. Bockfeld and M. Tamm, CCDC 2478753: Experimental Crystal Structure Determination, 2025, DOI: 10.5517/ccdc.csd.cc2p6bs1; (*i*) L. J. Groth, D. Bockfeld and M. Tamm, CCDC 2478754: Experimental Crystal Structure Determination, 2025, DOI: 10.5517/ccdc.csd.cc2p6bt2.